Available online at www.sciencedirect.com
ScienceDirect
International Journal of Heat and Mass Transfer 50 (2007) 2190–2199
International Journal of HEAT and MASS TRANSFER
www.elsevier.com/locate/ijhmt

Non-isothermal adsorption kinetics of water vapour into a consolidated zeolite layer

B. Dawoud [a,*], U. Vedder [a], E.-H. Amer [b], S. Dunne [c]

[a] Chair of Technical Thermodynamics, RWTH Aachen University, Schinkelstr. 8, D-52056-Aachen, Germany
[b] Department of Mechanical Power Engineering, Faculty of Engineering, El-Menoufiya University, Shebin El-Kom, Egypt
[c] UOP Molecular Sieves, 25 East Algonquin Road, P.O. Box 5017, Des Plaines, IL 60017-5017, USA

Received 25 April 2006; received in revised form 24 October 2006
Available online 27 February 2007

Abstract

A one-dimensional model for the kinetics of water vapour adsorption into a consolidated zeolite layer is presented. The combined heat and mass transfer problem is modelled and simulated using the software packet gPROMS® (general PROcess Modelling System). The centered finite difference method approximation is employed in solving the obtained set of partial differential, ordinary differential and algebraic model equations. Mass transfer is described by micro-pore diffusion, while heat transfer is described in terms of conduction. The temperature dependence of the diffusion coefficient is defined by an Arrhenius relationship, whereas the concentration dependence is accounted for by the Darken factor. The validity of the developed model has been checked against an experimental study, in which the kinetics of water vapour adsorption into a consolidated zeolite layer has been investigated in a constant volume-variable pressure test rig. The starting pressure has been changed in the range of 10–30 mbar, while the wall temperature has been adjusted to 35 and 50 °C. The measured characteristic half time for the adsorption kinetics varies between 13 and 21 s, while the required time to reach 90% of the equilibrium water loading lies between 70 and 94 s depending on the adsorption boundary condition. These times are quite short and promise highly compacted adsorption heat pump appliances. Fitting the results of the experimental investigations against the numerical simulation model gives a micro-pore diffusion coefficient (D_∞) of 1.58×10^{-4} ($m^2\,s^{-1}$) and an activation energy of 32.41 (kJ mol^{-1}). Furthermore, a measuring cell wall heat transfer coefficient (α_W) of 230 (W $m^{-2}\,K^{-1}$) has been estimated.

Keywords: Adsorption kinetics; Consolidated zeolite layer/gPROMS; Heat and mass transfer; Micro-pore diffusion; Zeolite-water

1. Introduction

Adsorption processes have been extensively studied for gas separation, catalysis, etc. At present, adsorption heat pumps (AHPs) represents one of the most promising technical applications of the adsorption process. They are thermally driven and can, therefore, make use of waste heat as well as thermal renewable energy resources. Moreover, AHPs can utilize high energy fuels more effectively than modern condensing boiler heating systems and, consequently, a reasonable amount of the resulted environmental pollution could be avoided. One of the most interesting working pairs for AHPs is zeolite-water. This working pair is non-poisonous, non-flammable and, moreover, has no ozone depletion potential.

The adsorption of water vapour into a porous solid adsorbent, such as zeolite, results in the release of the heat of adsorption. Accordingly, the temperature of the adsorbent particle rises, which reduces its water uptake capacity. Therefore, the heat of adsorption has to be removed before a further vapour mass transfer into the adsorbent particle may take place. Thus, the rate of vapour adsorption in zeolite is mainly controlled by both heat and mass transfer

* Corresponding author. Present address: Viessmann Werke GmbH & Co. KG, R&D "New Technologies" Viessmann Str. 1, D-35107 Allendorf/Eder, Germany. Tel.: +49 6452 703410; fax: +49 6452 706410.
E-mail address: DrDaw@Viessmann.com (B. Dawoud).

0017-9310/$ - see front matter © 2007 Elsevier Ltd. All rights reserved.
doi:10.1016/j.ijheatmasstransfer.2006.10.052

Nomenclature

A	cross-sectional area of the zeolite layer (m^2)
c	specific heat capacity (kJ kg^{-1} K^{-1})
D	micro-pore diffusion coefficient (m^2 s^{-1})
D_0	corrected diffusivity (m^2 s^{-1})
D_∞	diffusion coefficient at infinite temperature (m^2 s^{-1})
h	enthalpy (kJ kg^{-1})
E_a	activation energy (kJ mol^{-1})
$\dot{m}$	mass flow rate (kg s^{-1})
$\dot{m}''$	mass flux (mass flow rate per unit area) (kg s^{-1} m^{-2})
p	pressure (mbar)
q_{ads}	isosteric heat of adsorption (kJ kg^{-1})
R_m	universal gas constant (kJ mol^{-1} K^{-1})
S	thickness of zeolite layer (m)
t	time (s)
T	temperature (K)
u	specific internal energy (kJ kg^{-1})
V	volume (m^3)
x	water loading (kg/100 kg)
Z	spatial coordinate (m)

Greek symbols

α	heat transfer coefficient (W m^{-2} K^{-1})
λ	Thermal conductivity of zeolite layer (W m^{-1} K^{-1})
ρ	density (kg m^{-3})
χ	dimensionless differential water loading (−)

Superscript

l	liquid

Subscripts

dry	dry zeolite
0	initial value
∞	final value
v	vapour
V	volume
W	wall
w	water
wet	wetted zeolite
Zeo	zeolite

mechanisms within the pore network [1]. The evaluation of the heat and mass transfer rates accompanied with such an adsorption process is, therefore, a very important aspect in designing and optimizing the operation of an adsorption heat pump.

Based on certain simplifying assumptions, analytical solutions for the heat and mass transfer in fixed-bed operations have been obtained. To solve the cumbersome expressions involved, even for the simple isothermal adsorption processes, linear as well as non-linear adsorption equilibrium relations, based on Henry's and Langmuir's models, respectively, are assumed for these analytical solutions [2].

Because of the mathematical complexity associated with an exact description of intra-particle diffusion in spherical sorbent particles, approximate expressions have been formulated. The most widely used approximation is the Glueckauf linear driving force (LDF) approximation [3], which has been generalized later by Nakao and Suzuki [4]. An extension to the analysis of adsorption in spherical particles with diffusion taken as the sole factor in the process has been performed [5–7]. In these analyses, the Fourier series expansion, the Laplace transformation, and the penetration theory have been implemented to obtain the exact solution of that problem. Yao and Tien [8] have presented both the modified shell-core (MSC) model and the general driving force (GDF) model for evaluating the isothermal adsorption rate in an adsorbent pellet (which may be a slab, a cylinder or a sphere). Both the MSC and GDF models provide a reasonably good approximation to the exact solution presented in [5–7] while the LDF model is found to be a poor one in most situations.

One-dimensional studies of non-isothermal adsorption processes have also been performed. The suggested model by Brunovská et al. [9] includes heat transfer in an external film and mass transfer inside the porous structure. The gas phase diffusion is the only considered mass transfer mode and is described by means of Fick's law and the diffusivity is assumed to be independent on both concentration and temperature. Busweiler and Kast [10] have presented a model for the combined heat and mass transfer in a single adsorption pellet. The model comprises the diffusion as well as the Knudsen molecular motion as the mass transfer modes in the gas phase and surface diffusion as the corresponding mode in the adsorbed phase at higher concentrations. The heat is assumed to be transferred by conduction through the solid phase. The measured data have been fitted to the model resulting in mean values for the mass transfer coefficients. With these coefficients, a fairly good agreement between the measured and the calculated temperature as well as water loading on silica gel was obtained.

Two- and three-dimensional studies of the momentum, heat and mass transfer problem of the adsorption/desorption of water vapour in a 13X-zeolite packed-bed have been carried out [11,12]. Mhimid [11] has investigated the validity of the local thermal equilibrium assumption between the gas phase and the adsorbent during desorption of water. He concluded that this assumption is not valid and a non-equilibrium model has to be used to determine the amount of desorbed water. In the model of Zhang and Wang [12] a linear driving force equation is used to account for mass-transfer resistance within the pellets, while Darcy's law is introduced to describe the adsorbate flows in the inter-particle voids.

In a previous work Dawoud et al. [13] presented a one-dimensional dynamic model for the kinetics of water vapour adsorption into a zeolite layer, in the working range of adsorption heat pumps. The mass transfer has been described in terms of Knudsen diffusion. The validity of the model has been tested against one kinetic measurement on a consolidated layer of NaA-zeolite giving good agreement.

In this communication, measurements on the kinetics of water vapour adsorption into a consolidated adsorbent layer made of Molsiv™ DDZ-70 [14] have been carried out in a constant-volume variable-pressure kinetic setup. The starting pressure has been varied between 10 and 30 mbar, while the wall temperature of the measuring cell, on which the adsorbent layer sample is placed, has been adjusted to 35 and 50 °C. The obtained experimental results have been discussed and compared. Moreover, a dynamic model has been set up to simulate the combined heat and mass transfer during the considered non-isothermal adsorption process. Mass transfer has been described by Darken-corrected [15] micro-pore diffusion. The temperature dependence of the diffusion coefficient is described in terms of an Arrhenius relation. The simulations have been carried out with the software packet gPROMS® [16]. The obtained experimental results have been fitted to the simulation model to estimate the micro-pore diffusion coefficient, the activation energy and the overall heat transfer coefficient between the bottom of the zeolite layer and the wall of the measuring cell.

2. The kinetic setup

Fig. 1 depicts schematically the constant-volume variable-pressure setup for measuring the kinetics of water vapour adsorption. The setup consists mainly of a measuring cell and a vapour vessel. The cell and the vessel are connected by a pipe, which can be locked by a valve. The zeolite sample is placed onto the isothermal wall of the measuring cell.

The temperatures of the cell and the vapour vessel are adjusted by oil and water loops, which are controlled by the thermostatic bathes 2 and 1, respectively. In order to activate the sample the measuring cell is tempered at 150 °C and evacuated simultaneously for 2 h. During this desorption process the regulating valve (RV) is kept closed while the valves V1–V3 are opened. The water loading at the end of this activation process is determined by performing thermogravimetrical tests on the sample under same boundary conditions (150 °C and 10^{-2} mbar for 2 h).

Both valves V2 and V3 are then closed and the temperature of the oil loop is adjusted to the required adsorption temperature (35 or 50 °C). Before starting an experiment, water vapour from the steam generator is charged into the vessel to a certain starting pressure, which is higher than the prevailing vapour pressure of the remaining adsorbed water in the zeolite sample in the measuring cell (thermodynamic non-equilibrium). The course of pressure decrease with time due to adsorption, after opening the valve (V2), which is measured by the two pressure gauges P1 and P2 in Fig. 1, determines the kinetics of the adsorption process. More details about the setup, the experimental procedure and the evaluation routine for the measured data can be read in Dawoud and Aristov [17].

Table 1 summarizes the characteristics of the setup as well as the boundary conditions for the experimental investigations.

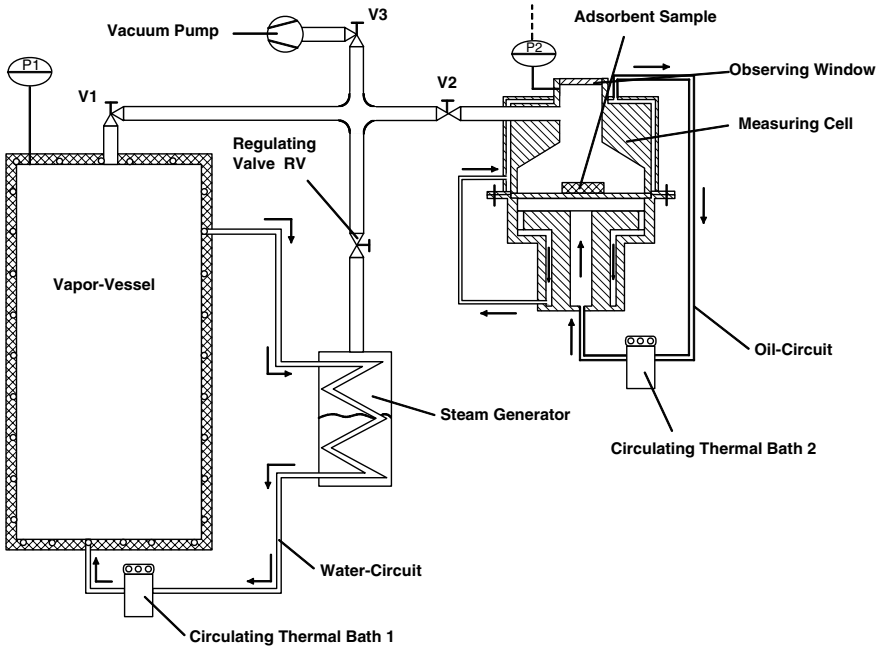

Fig. 1. Setup for measuring the kinetics of water vapour adsorption.

Table 1
Setup characteristics and experimental parameters

Initial water loading	$x_0 = 1.4$ kg/100 kg
Total mass of dry sample	3.75 g
Start pressure range	10–30 mbar
Wall temperature	50/35 °C
Volume of the measuring cell	$V_{MZ} = 0.74$ L
Volume of the vapour vessel	$V_B = 23.73$ L

The tested zeolite layer has been coated on an aluminum substrate with a thickness of 0.55 mm and a diameter of 98.5 mm. The zeolite coated layer is a UOP technology using a polymer binder to form a cast film of zeolite. The mass of pure zeolite in the layer amounts to 3.0 g and the thickness of the layer is 0.7 mm.

3. Mathematical model

In this section, the set of equations describing the model of the combined heat and mass transfer in a consolidated zeolite layer will be illustrated. Fig. 2 shows the discretisation of the zeolite layer. The following basic assumptions were made:

1. The heat and mass transfer problem is considered to be one-dimensional.
2. All infinitesimally small zeolite sub-layers are considered to be phases in thermodynamic equilibrium.
3. The heat content of the vapour phase within the zeolite structure can be neglected as the density ratio between vapour and liquid phase is very small. At the working temperature and pressure of e.g. 100 °C and 100 mbar, the density ratio between vapour and liquid is approximately 5.0×10^{-5}.
4. The zeolite layer and the adsorbed water are considered to be incompressible.

3.1. Energy balance

The energy balance for the zeolite layer, including the diffusive enthalpy rate of the absorbed vapour, can be formulated according to Bosnjakovic and Knoche [18] as follows:

$$\frac{\partial}{\partial t}(\rho_{zeo}(x)\cdot u(x,T)) = \frac{\partial}{\partial z}\left(\lambda\cdot\frac{\partial T}{\partial z}\right) - \frac{\partial}{\partial z}(\dot{m}''_v\cdot h_v) \quad (1)$$

where $u(x,T)$ represents the specific internal energy of wetted zeolite, which is a function of both the water loading x and the prevailing zeolite temperature T, and $\dot{m}''_v$ is the mass flux of the adsorbed water vapour. The temperature dependence of the internal energy is expressed in terms of the specific heat capacity of water loaded zeolite, while the water loading dependence is represented by the partial differential internal energy of the adsorbed water. The partial differential internal energy is defined, for an incompressible adsorption system, as the difference between the enthalpy of water vapour and the differential isosteric heat of adsorption (Dawoud [19]).

3.2. Mass balance

According to Busweiler and Kast [10] the continuity equation for each sub-layer can be formulated as follows:

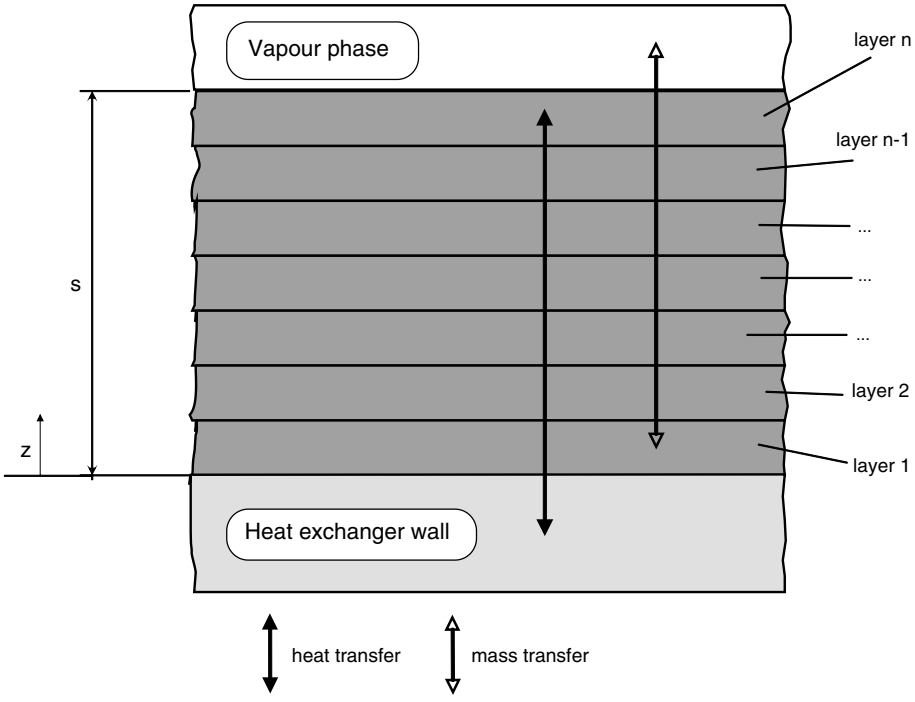

Fig. 2. Discretisation of the zeolite layer.

$$\frac{\partial \rho}{\partial t} = -\frac{\partial \dot{m}''_v}{\partial z} \tag{2}$$

Neglecting the volume of the adsorbed water in zeolite, the density of the water loaded zeolite (ρ) can be expressed as

$$\rho_{zeo} = \rho_{zeo,dry} \cdot (1 + x/100) \tag{3}$$

where $\rho_{zeo,dry}$ is the density of dry zeolite and amounts to 703.6 kg/m^3 according to the manufacturer (UOP).

Combining the energy and mass balance equations (1) and (2) with Eq. (3) and the definitions given by Dawoud [19] for the specific internal energy of wetted zeolite, Vedder [20] came up with the following expression for the energy balance of each infinitesimal zeolite sublayer

$$\rho_{zeo} \cdot \left(c_{zeo,wet} \cdot \frac{dT}{dt} - q_{ads} \cdot \frac{dx}{dt} \right) = \frac{\partial}{\partial z}\left(\lambda \cdot \frac{\partial T}{\partial z} \right) - \dot{m}''_v \cdot \frac{\partial h_v}{\partial z} \tag{4}$$

where $c_{zeo,wet}$ and q_{ads} are the specific heat capacity of wetted zeolite and the isosteric heat of adsorption, respectively.

3.3. Conservation of mass in the vapour phase

The time rate of water vapour mass reduction, in the vapour vessel as well as in the measuring cell, is equal to the adsorbed mass flow rate of water vapour on the top of the zeolite layer. With A representing the surface area of the zeolite layer, this can be expressed as

$$\frac{\partial m_v}{\partial t} = -\dot{m}''_v(S) \cdot A \tag{5}$$

The ideal gas behaviour is assumed for the water vapour phase

$$p_v \cdot V_v = m_v \cdot R_v \cdot T_v \tag{6}$$

3.4. Mass transfer

Micro-pore diffusion takes place when the pore diameter is in the same order of magnitude of the dimensions of the diffusing molecule. According to Ruthven [1] the diffusive mass flow rate can be written as

$$\dot{m}_v = -A \cdot D \cdot \rho_{zeo} \cdot \frac{\partial x}{\partial z} \tag{7}$$

Herein A is the surface area of the adsorbent layer and D is the micro-pore diffusion coefficient, which is usually referred to as the "Fickian diffusivity". Fick's first law carries the implication that the driving force for diffusion is the gradient of concentration. However, since diffusion is simply the macroscopic manifestation of the tendency to approach equilibrium, it is clear that the true driving force must be the gradient of chemical potential [15]. Accordingly, the diffusive flux can be considered as a flow driven by the gradient of chemical potential and opposed by frictional forces. Following this concept, Kärger and Ruthven [15] have developed the following relation for the micro-pore diffusion coefficient in case of the diffusion of a single component in a porous adsorbent:

$$D = D_0 \cdot \left. \frac{d \ln p}{d \ln x} \right|_T \tag{8}$$

The micro-pore diffusion coefficient D or the "Fickian diffusivity" is thus the product of the self diffusion (mobility) coefficient D_0 or the "corrected diffusivity" and the thermodynamic correction factor according to Darken [21]. The Darken factor $(d \ln p/d \ln x)_T$ is the inverse of the slope of the equilibrium adsorption isotherm of the pure gas. If the system is thermodynamically ideal ($p \propto x$), then $d \ln p/d \ln x \to 1.0$ and the Fickian and the corrected diffusivities become identical. Thermodynamic ideality is generally approached only in dilute systems and, under these conditions, one may also expect negligible interaction between the diffusing molecules, leading to a diffusivity that is independent of concentration. In fact, except in dilute systems, the Fickian diffusivity is generally concentration dependent. Eq. (8) shows that this dependence may arise from the concentration dependence of either D_0 or $d \ln p/d \ln x$. For adsorption systems and near the saturation region the equilibrium isotherm becomes almost horizontal so that $d \ln p/d \ln x \to 0$ whereas in the low concentration (Henry's Law) region $d \ln p/d \ln x \to 1.0$. The concentration dependence of the thermodynamic correction factor is found to be much more pronounced than the concentration dependence of the corrected diffusivity [15]. The diffusive mass flux in case of micro-pore diffusion can then be written as

$$\dot{m}''_v = -\rho_{zeo} \cdot D_0 \cdot \left. \frac{d \ln p}{d \ln x} \right|_T \cdot \frac{\partial x}{\partial z} \tag{9}$$

The temperature dependence of the corrected diffusivity (D_o) is described by an Arrhenius relationship as

$$D_0 = D_\infty \cdot \exp(-E_a/(R_m \cdot T)) \tag{10}$$

where D_∞ and E_a represent the diffusivity at infinite temperature and the activation energy, respectively.

3.5. Boundary and initial conditions

3.5.1. Boundary conditions

3.5.1.1. Heat transfer. The heat transfer from the bottom of the zeolite layer to the wall of the measuring cell being kept at a constant temperature T_W is assumed to take place with an overall wall heat transfer coefficient (α_W). The value of the overall heat transfer coefficient is to be estimated through fitting the experimental data to the simulation model. Eq. (11) defines the heat transfer boundary condition at the bottom of the zeolite layer.

$$-\lambda \cdot \left. \frac{\partial T}{\partial z} \right|_{z=0} = \alpha_W \cdot \left(T_W - T|_{z=0} \right) \tag{11}$$

The energy exchange between the uppermost zeolite sub-layer and the vapour phase is assumed to be only due to the diffusive enthalpy flow of the adsorbed water vapour. In other words, the heat transfer by convection as well as radiation with the vapour phase is neglected. This is justified by the fact that the molecules of water vapour close to the uppermost sub-layer, which may be heated by convection or radiation, are those which will be directly adsorbed in the subsequent time interval. Accordingly, the relevant boundary condition to the energy equation can be formulated as

$$\left.\frac{\partial T}{\partial z}\right|_{z=S} = 0 \tag{12}$$

3.5.1.2. Mass transfer. Regarding the mass transfer within the zeolite layer, it is assumed that there is no mass transfer from the bottom of the zeolite layer. The pressure of the vapour phase is set equal to the pressure at the uppermost segment of the zeolite layer. Accordingly, the following two boundary conditions can be formulated for the mass transfer

$$\left.\frac{\partial x}{\partial z}\right|_{z=0} = 0 \tag{13}$$

$$p|_{z=S} = p_v \tag{14}$$

3.5.2. Initial conditions

The zeolite layer is assumed to have initially a homogeneous temperature and water loading, and accordingly, homogeneous equilibrium vapour pressure distribution.

3.6. Thermal and calorific properties

According to the second assumption, all infinitesimally small zeolite sub-layers are considered to be phases in thermodynamic equilibrium. The adsorption equilibrium data of the considered adsorbent/adsorbate pair (MOLSIV™ DDZ-70/water) is described by the following equilibrium equation:

$$\ln p = A(x) + \frac{B(x)}{T} \tag{15}$$

Herein the parameters $A(x)$ and $B(x)$ are functions of the water loading (x) according to the following equation:

$$A(x) = a_0 + a_1 x + a_2 x^2 + a_3 x^3 \tag{16}$$

$$B(x) = b_0 + b_1 x + b_2 x^2 + b_3 x^3 \tag{17}$$

The parameters a_n and b_n with $\{n \in N | 0 \leqslant n \leqslant 3\}$ have been obtained by fitting our own equilibrium data to the isosteric equilibrium model defined by Eqs. (15)–(17) and are listed in Table 2.

The isosteric heat of adsorption q_{ads} can be described in terms of Eq. (18) according to Kast [2] where R_v is the gas constant of the adsorbate

$$q_{ads} = -R_v \cdot B(x) \tag{18}$$

Table 2
Parameters of the equilibrium function (Eqs. (16) and (17))

a_0	17.22	b_0	−6887.1
a_1	0.1638	b_1	341.58
a_2	0.0127	b_2	−32.005
a_3	0.0005	b_3	0.8676

The specific heat capacity of the wetted zeolite ($c_{zeo,wet}$) is expressed as a superposition of the specific heat capacities of dry zeolite and the bulk adsorbate according to Eq. (19)

$$c_{zeo,wet} = c_{zeo,dry} + x \cdot c_w^l \tag{19}$$

According to the manufacturer (UOP), the thermal conductivity of the zeolite DDZ-70 amounts to 0.208 W m^{-1} K^{-1}.

4. Solution method

The model equations expressed above are co-ordinate and time dependent. To consider the co-ordinate dependency, the zeolite layer is discretised into balance elements in the Z-direction (Fig. 2). The gPROMS package has been used for the system modelling and simulation. The system of partial differential and algebraic equations (PDAEs) presented above is written directly in gPROMS using its high-level modelling language and is then solved using the method of lines family of numerical methods. This involves the automatic discretisation of the distributed equations with respect to all spatial domains, which results in mixed sets of time-dependent ordinary differential and algebraic equations (DAEs). The resulting DAE system is then solved by gPROMS' built-in DAE solver. In this paper, among the various discretisation techniques available with gPROMS, the centered finite difference (CFDM) is applied. The gPROMS's parameter estimation tool (gEST) has been applied to fit the measured experimental data to the simulation model, resulting in the values of the diffusion coefficient, the activation energy and the wall heat transfer coefficient of the measuring cell.

5. Results and discussion

In this section the results of the experimental investigations as well as simulations of the kinetics of water vapour adsorption onto a consolidated zeolite layer MOLSIV™ DDZ-70 in a constant-volume, variable-pressure setup will be presented. The kinetic measurements have been carried out at two different measuring cell wall temperatures; namely, 35 and 50 °C and three starting vapour pressures; namely, 10, 20, and 30 mbar. The main goal of the simulation work was to estimate the diffusion coefficient (D_∞), the activation energy (E_a) and the wall heat transfer coefficient (α_W) of the measuring cell. Moreover, the obtained simulation data on the time course of variation of the average zeolite layer temperature have been applied to explain the measured adsorption kinetic data.

5.1. Experimental results

Fig. 3 depicts the obtained experimental results of the absolute water loading variation with time depending on the tested boundary conditions.

It can be simply noticed that the higher the measuring cell wall temperature and, consequently, the final adsorption temperature, the lower the equilibrium water loading. This is clear as the adsorption capacity of an adsorbent becomes lower at higher temperatures. Moreover, the difference in the equilibrium water loading between the tested two temperatures becomes higher as the starting water vapour pressure increases. Recalling that the measuring system has a constant volume, this tendency becomes also clear as the available water vapour mass for the adsorption process increases with increasing the starting pressure. Indeed the equilibrium state is reached first after 2 h. The time axis of Fig. 3 has been shortened, only, to show the most interesting time phase of the kinetic process. Table 3 gives the obtained equilibrium water loadings (x_∞) for the tested boundary conditions.

In order to compare the results of measuring the adsorption kinetics under different operating conditions, it is reasonable to represent the time variation of the water loading in a dimensionless form. This may occur by defining the dimensionless differential water loading χ as the ratio between the instantaneous differential water loading to the maximum differential water loading achievable at each operating condition of the adsorption process on the adsorbent sample:

$$\chi(t) = \frac{x(t) - x_0}{x_\infty - x_0}. \tag{20}$$

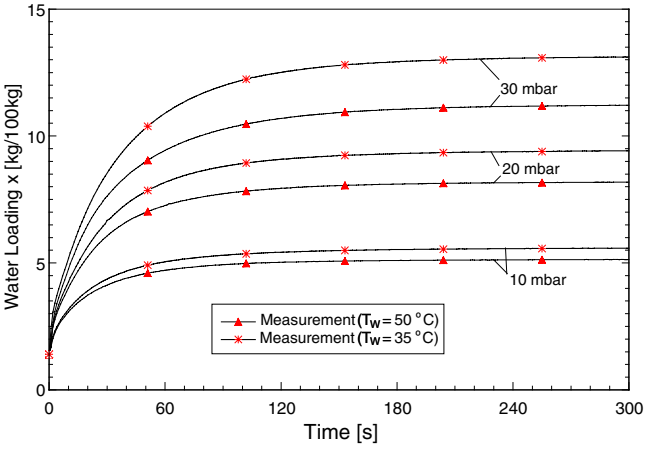

Fig. 3. Absolute water loading against time for the tested boundary conditions.

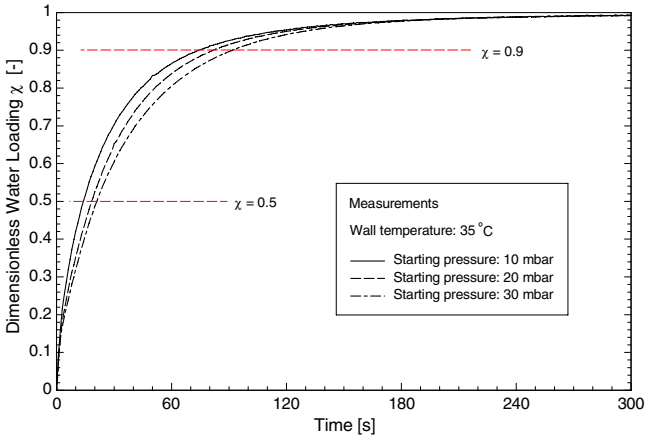

Fig. 4. Dimensionless differential water loading against time for the measuring cell wall temperature of 35 °C.

Fig. 4 depicts exemplarily the kinetic curves of water sorption at a constant measuring cell temperature of 35 °C in a "dimensionless differential water loading versus time" presentation. Due to the non-linearity of the adsorption isotherms as well as the temperature increase of the zeolite sample, there is no analytical model existing, according to which the diffusion coefficient of such an adsorption process can be estimated. Accordingly, the obtained adsorption rates were characterized by times $\tau_{\chi=0.5}$ and $\tau_{\chi=0.9}$ for reaching 50% and 90% of the equilibrium loading. The characteristic time $\tau_{\chi=0.5}$ is the measure for the adsorption kinetics, while the time $\tau_{\chi=0.9}$ is a good estimation for the half-cycle time of an adsorption heat pump, as waiting for equilibrium ($\chi = 1.0$) will result in decreasing the average power sharply. Table 3 gives also the two characteristic times for the measured boundary conditions. The characteristic time for the adsorption kinetics varies between 13 and 21 s, while the required time to reach 90% of the equilibrium water loading lies between 70 and 94 s depending on the adsorption boundary condition. These times are quite short and promise highly compacted adsorption heat pump appliances.

Table 3
Measured equilibrium water loadings and characteristic times at the different adsorption boundary conditions

p_0 (mbar)	$T_W = 35$ °C			$T_W = 50$ °C		
	x_∞ (kg/100 kg)	$\tau_{\chi=0.5}$ (s)	$\tau_{\chi=0.9}$ (s)	x_∞ (kg/100 kg)	$\tau_{\chi=0.5}$ (s)	$\tau_{\chi=0.9}$ (s)
10	5.6	14	74	5.2	13	70
20	9.5	18	82	8.3	16	76
30	13.2	21	94	11.3	19	92

Moreover, it can be noticed that the lower the starting pressure, the faster the adsorption process. At lower starting pressures, the amount of water adsorbed is less and, consequently, the released heat of adsorption is also less. This explains why the combined heat and mass transfer process requires more time if the starting pressure increases. Despite the enhancement of water diffusivity with the average layer temperature enhancement, resulting from the release of more heat of adsorption, it is obvious that the heat transfer characteristics dominate the combined process. The temperature development in the zeolite layer under different adsorption boundary conditions will be explained at the end of the simulation part, which will very much help in clearing the described thermal effects.

Furthermore, the adsorption kinetics at the measuring cell's wall temperature of 50 °C are slightly faster than those at 35 °C. This can be partially attributed to the less amount of water adsorbed at 50 °C. On the other hand, this can be explained by the increase of water diffusivity as the average process temperature increases.

5.2. Simulation results

Fig. 5 depicts the experimental and simulation results of the mean water loading against time for the starting pressures 10, 20 and 30 mbar and the measuring cell wall temperature of 50 °C. The simulations have been carried out with a constant micro-pore diffusion coefficient. It can be simply observed that only the measured data at a starting pressure of 10 mbar could be fitted well to the simulation results. With a Fickian diffusivity (D in Eq. (7)) of 1.75×10^{-9} m^2 s^{-1} the simulation results fit the measured data very well (relative deviation <0.8%). Comparing the measured data at the adsorption temperature of 50 °C and the starting pressures of 20 and 30 mbar (Fig. 5) to those estimated with the same value of the Fickian diffusivity reveals good (maximum relative deviation of ±4.1%) and fair (maximum relative deviation of ±7.4%) agreements, respectively. Schnabel and Henning [22] have got poor agreements between simulated and measured kinetic data by applying a constant "effective" diffusion coefficient to describe the adsorption of water vapour onto a similar consolidated zeolite layer.

It is clear that a constant micro-pore diffusion coefficient can only describe the adsorption kinetics in the region, where Henry's Law is valid, i.e. in the low concentration region. It can, therefore, be concluded that for the tested zeolite-water system, a constant micro-pore diffusion coefficient can describe well the adsorption kinetics up to a water loading of 5 g/100 g. Moreover, both temperature and water loading dependences of the diffusion coefficient have to be taken into account. This has been carried out according to Eqs. (8)–(10). The results are explained within the following paragraphs.

Figs. 6 and 7 illustrate the measured kinetic curves of the mean water loading in comparison with the simulation results for the measuring cell wall temperatures of 50 and 35 °C, respectively. In the simulations the water loading dependence of the diffusion coefficient has been taken into account through Eq. (8), while the temperature dependence through Eqs. (9) and (10). Using the parameter estimation tool of the applied software "gPROMS" to fit the measured data to the simulation model, results in a wall heat transfer coefficient (α_W) of 230 W m^{-2} K^{-1}, a micro-pore diffusion coefficient at infinite temperature (D_∞) of 1.58×10^{-4} m^2 s^{-1} and an activation energy (E_a) of 32.41 kJ mol^{-1}.

As depicted in Figs. 6 and 7 the estimated kinetic data fit quite well to the measured curves with an average deviation of ±1.4% and ±3.9% at the measuring cell wall temperatures of 50 and 35 °C, respectively.

Finally, the simulation model has been applied to estimate the mean zeolite temperature (averaged over the zeolite layer height) under different adsorption boundary conditions, in order to explore the intensity of the thermal effects, resulting from the release of the heat of adsorption and to support the interpretation of the experimental data presented in Fig. 4. The time variation of the mean zeolite

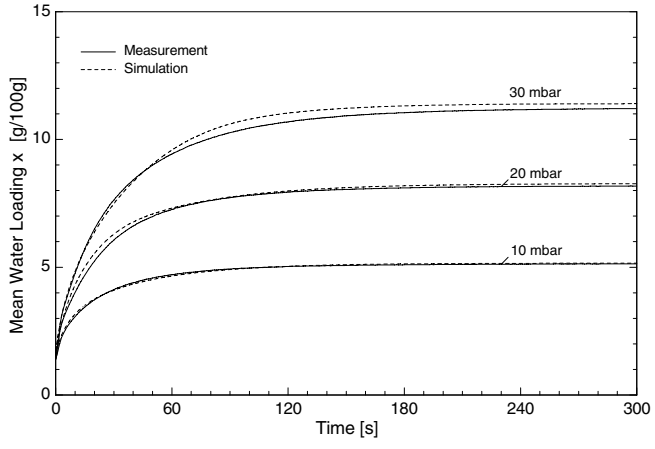

Fig. 5. Measured and simulated water loadings with a constant micro-pore diffusion coefficient at a measuring cell wall temperature of 50 °C.

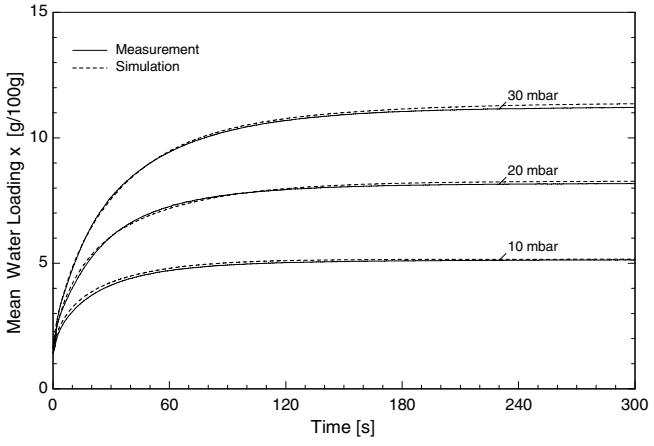

Fig. 6. Measured and simulated water loadings with a Darken-corrected micro-pore diffusion coefficient at a measuring cell wall temperature of 50 °C.

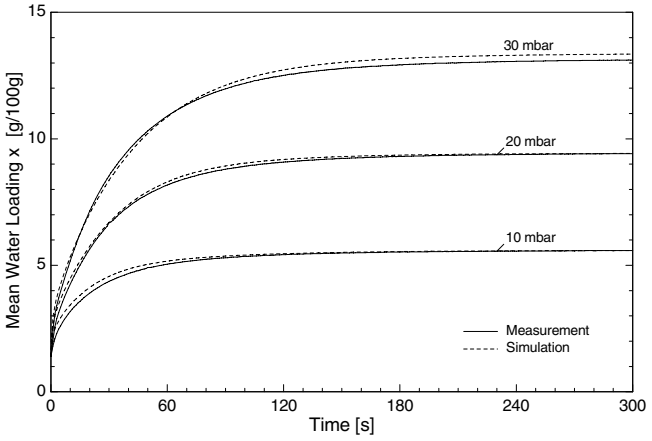

Fig. 7. Measured and simulated water loading curves with a Darken-corrected micro-pore diffusion coefficient at a measuring cell wall temperature of 35 °C.

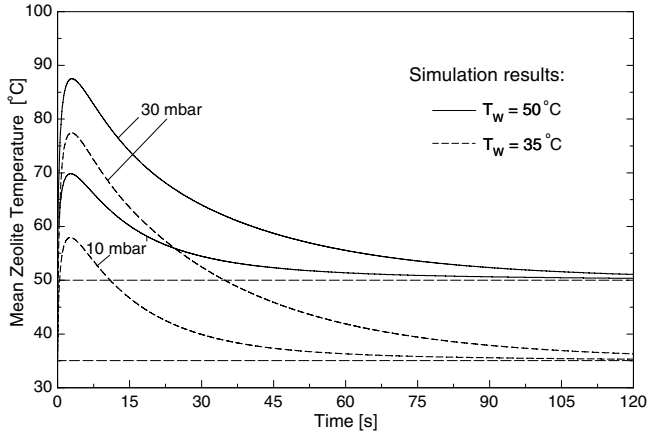

Fig. 8. Simulated mean zeolite temperatures at different measuring cell wall temperatures and starting pressures.

temperature for two starting pressures (10 and 30 mbar) and two measuring cell wall temperatures (35 and 50 °C) is depicted in Fig. 8. It can be observed that the mean zeolite temperature attains a maximum which increases with the starting pressure. Beyond this maximum the mean zeolite temperature decays and approaches the wall temperature within 2–3 min. At a starting pressure of 10 mbar, a temperature increase of 20 K is estimated at T_W equals 50 °C versus a temperature increase of 23 K at T_W equals 35 °C. These values go up to 37 and 42 K, respectively, at the starting pressure of 30 mbar. As a first approximation, the area under each temperature curve is indeed proportional to the amount of heat released in the zeolite layer, which is obviously more for the wall temperature of 35 °C. This can be explained by the fact that the initial mass transfer driving force (concentration gradient between the gas phase and the mean equilibrium concentration in the zeolite layer) is higher for $T_W = 35$ °C. Consequently, the initial adsorbed amount and the amount of heat released is higher.

6. Conclusion

A one-dimensional model for the dynamics of the combined heat and mass transfer during the adsorption of water vapour into a consolidated zeolite "MOLSIV™ DDZ-70" layer has been presented. The model is utilized to simulate a constant-volume adsorption kinetic setup as well as to estimate the diffusion coefficient and the measuring cell wall heat transfer coefficient. Adsorption kinetic measurements have been carried out at starting pressures of 10, 20 and 30 mbar and measuring cell wall temperatures of 35 and 50 °C. Micro-pore diffusion with constant as well as Darken-corrected diffusion coefficients have been applied. The temperature dependence of the micro-pore diffusion coefficient is described in terms of an Arrhenius type equation. Heat transfer is described by conduction. It turned out that a constant micro-pore diffusion coefficient is only capable to describe the diffusion in the low concentration region (below 5 g/100 g). The Darken-corrected micro-pore diffusion coefficient depicts the concentration dependence of the diffusion coefficient quite well. Fitting the measured data to the simulation model, results in a measuring cell wall heat transfer coefficient (α_W) of 230 W m^{-2} K^{-1}, a micro-pore diffusion coefficient at infinite temperature (D_∞) of 1.58×10^{-4} m^2 s^{-1} and an activation energy (E_a) of 32.41 kJ mol^{-1}.

References

[1] D.M. Ruthven, Principles of Adsorption and Adsorption Processes, John Wiley and Sons, 1984.
[2] W. Kast, Adsorption aus der Gasphase; Ingenierwissenschaftliche Grundlagen und technische Verfahren, VCH-Verlagsgesellschaft mbH, 1988.
[3] E. Glueckauf, Theory of chromatography, Part X. Formulae for diffusion into spheres and their application to Chromatography, Trans. Faraday Soc. 51 (1955) 1540–1551.
[4] S.-I. Nakao, M. Suzuki, Mass transfer coefficient in cyclic adsorption and desorption, J. Chem. Eng. Jpn. 16 (2) (1983) 114–119.
[5] E. Alpay, D.M. Scott, The linear driving force model for fast-cycle adsorption and desorption in a spherical particle, Chem. Eng. Sci. 47 (1992) 499–502.
[6] G. Carta, The linear driving force approximation for cyclic mass transfer in spherical particles, Chem. Eng. Sci. 48 (1993) 622–625.
[7] D.M. Scott, The linear driving force model for cyclic adsorption and desorption: the effect of shape, Chem. Eng. Sci. 49 (1994) 914–916.
[8] C.C. Yao, C. Tien, Application of new rate models to cyclic adsorption in adsorbents, Chem. Eng. Sci. 53 (1998) 3763–3766.
[9] A. Brunovská, I. Ilavský, V. Hlavácek, An analysis of a nonisothermal one-component sorption in a single adsorbent particle – a simplified model, Chem. Eng. Sci. 36 (1981) 123–128.
[10] U. Busweiler, W. Kast, Nichtisotherme Ad- und Desorptionskinetik am Beispiel der Wasserdampfadsorption an Einzelkörnen technischer Adsorbentien, Chem.-Ing.-Tech. 56 (11) (1984) 860–861.
[11] A. Mhimid, Theoretical study of heat and mass transfer in a zeolite bed during water desorption: validity of local thermal equilibrium assumption, Int. J. Heat Mass Transfer 41 (1998) 2967–2977.
[12] L.Z. Zang, L. Wang, Momentum and heat transfer in the adsorbent of a waste-heat adsorption cooling system, Energy 24 (1999) 605–624.
[13] B. Dawoud, T. Miltkau, A. Assefa, Combined heat and mass transfer analysis of the kinetics of water vapor adsorption into a zeolite layer, in: ISHPC '02, Proceedings of the International Sorption Heat Pump Conference Shanghai, China, September 24–27, 2002, pp. 595–602.

[14] B. Dawoud, S. Dunne, R. Lang, Experimental investigations of the kinetics of water vapor adsorption into MOLSIV™ DDZ-70 under typical operating conditions of adsorption heat pumps, in: ISHPC '02, Proceedings of the International Sorption Heat Pump Conference Shanghai, China, September 24–27, 2002, pp. 603–608.
[15] J. Kärger, D.M. Ruthven, Diffusion in Zeolites, Wiley-Interscience, New York, 1992.
[16] Process System Enterprise Limited, www.psenterprise.com/gPROMS.
[17] B. Dawoud, Y. Aristov, Experimental study on the kinetics of water vapor sorption on selective water sorbents, silica gels and alumina under typical operating conditions of sorption heat pumps, Int. J. Heat Mass Transfer 46 (2003) 273–281.
[18] F. Bosnjakovic, K.F. Knoche, Technische Thermodynamic – Teil 2, 6th ed., Steinkopf Verlag, Darmstadt, Germany, 1997.
[19] B. Dawoud, Thermische und Kalorische Stoffdaten des Stoffsystems Zeolith MgNaA-Wasser, Ph.D. Dissertation, RWTH-Aachen, Germany, 1999.
[20] U. Vedder, Nichtisotherme Adsorptionskinetik von Wasserdampf an einer kompakten Zeolithschicht, Dipl.-Ing. Thesis, Lehrstuhl für Technische Thermodynamik, RWTH Aachen University, Aachen, Germany, 2003.
[21] L.S. Darken, Diffusion: nobilities and their interrelation through free energy in Binary Metallic Systems, Trans. AIME 175 (1948) 184–201.
[22] L. Schnabel, H.-M. Henning, Experimental and simulation study on the kinetics of water vapor adsorption on different kinds of adsorptive material matrices, in: Proceedings of the International Conference on Sorption Heat Pumps, ISHPC05, June 22–24, Denver, CO, USA, Paper No. 39, 2005, pp. 1–8.